Journal of Applied Polymer Science

In-process thermochemical analysis of *in situ* poly(ethylene glycol methacrylate-*co*-glycidyl methacrylate) monolithic adsorbent synthesis

Caleb Acquah,[1,2] Michael K. Danquah,[1,2] Charles K. S. Moy,[3] Clarence M. Ongkudon[4]

[1]Curtin Sarawak Research Institute, Curtin University, Sarawak 98009 Malaysia
[2]Department of Chemical Engineering, Curtin University, Sarawak 98009 Malaysia
[3]Department of Civil Engineering, Xi'an Jiaotong-Liverpool University, Jiangsu 215123, China
[4]Biotechnology Research Institute, Universiti Malaysia Sabah, Kota Kinabalu, Sabah 88400 Malaysia
Correspondence to: M. K. Danquah (E-mail: mkdanquah@curtin.edu.my)

ABSTRACT: Thermomolecular mechanisms associated with the synthesis of polymethacrylate monoliths are critical in controlling the physicochemical and binding characteristics of the adsorbent. Notwithstanding, there has been limited reported work on probing the underlining synthesis mechanism essential in establishing the relationship between in-process polymerization characteristics and the physicochemical properties of the monolith for tailored applications. In this article, we present a real-time thermochemical analysis of polymethacrylate monolith synthesis by free-radical polymerization to probe the effects on the physicochemical characteristics of the adsorbent. The experimental results show that an increase in the crosslinker monomer concentration from 30 to 70% resulted in a peak temperature increase from 96.3 to 114.3 °C. Also, an increase in the initiator (benzoyl peroxide) concentration from 1 to 3% w/v resulted in a temperature increase from 90.7 to 106.3 °C. A temperature buildup increases the kinetic rate of intermolecular collision associated with microglobular formation and interglobular interactions. This reduces the structural homogeneity and macroporosity of the polymer matrix. A two-phase reactive crystallization model was used to characterize the rate of monomeric reaction after initiation and microglobular formation from the liquid monomeric phase to formulate the theoretical framework essential for evaluating the kinetics of the polymer formation process. © 2016 Wiley Periodicals, Inc. J. Appl. Polym. Sci. **2016**, *133*, 43507.

KEYWORDS: copolymers; porous materials; properties and characterization; radical polymerization; thermal properties

Received 20 November 2015; accepted 31 January 2016
DOI: 10.1002/app.43507

INTRODUCTION

Conventional chromatographic supports for bioseparation and purification in life sciences are generally particulate in nature, with small particle pores that present significant bioprocess challenges, especially for large-molecule applications, including plasmid DNA, viral particles, and cellular targets. The mode of mass transfer in particulate adsorbents is mostly diffusion, and this significantly slows down the flow hydrodynamics and reduces the mass velocity and capacity of matter into and out of the adsorbent. In addition, the random packing assembly of particulate adsorbents in chromatographic columns make it challenging to fine-tune its physical features for high throughput and rapid bioseparation applications.

Monolithic adsorbents are regarded as relatively new chromatographic stationary supports and are synthesized by various chemomolecular techniques to form a single piece of continuous sorbent in an unstirred mold.[1–3] Monoliths have the trademark of offering a convective mass transport of fluids and a low column backpressure as a result of their macroporous nature.[4] Their pore characteristics and surface functionalities can also be molecularly engineered to target analytes with various physicochemical properties, such as the hydrodynamic size, charge, and active moieties.[5–7] There are three main types of monoliths: organic, inorganic, and hybrid organic–inorganic monoliths. Organic monoliths, especially polymethacrylates, represent one of the most used monolithic adsorbents for chromatographic applications. They are largely pH resistant and biocompatible with easily tailored pore characteristics and readily available reactive moieties, such as epoxy groups, for functionalization.[8–10] Polymethacrylate monoliths are synthesized via the free-radical copolymerization of a crosslinker and functional methacrylate-based monomers that is initiated either thermally or by radiation.[11–13] The thermal initiation approach is commonly used, as it is cheap and primarily requires the use of an isothermal water bath.[14,15] The synthesis process includes various steps of thermomolecular mechanisms involving the monomers and the initiator. These steps are:

© 2016 Wiley Periodicals, Inc.

1. Sensible heat transfer from the heating medium to the polymerization mixture.
2. Decomposition of the initiator at its degradation temperature (T_i). This results in the release of exotherms and an increase in the temperature.
3. Reactive monomeric interactions driven by the released free radicals to form a nucleic complex in the liquid phase.
4. Formation of the solid polymer out of the liquid phase through microglobule development from the nuclei.

In each of these steps, the control of the physicochemical characteristics is important; hence, an in-depth understanding of the phenomenon is important in the development of well-characterized monoliths for targeted applications. However, current research efforts have mostly focused on bulk synthesis, characterization, functionalization, and chromatographic application[16–19] with a limited focus on the understanding of the molecular mechanisms governing the monolith formation process. This limits opportunities to fully exploit the adsorbent properties to enhance chromatographic performance indicators. Both in-process and postpolymerization characterizations are essential in tailoring the physicochemical properties of the adsorbent, widening the scope of application, and also tackling common challenges related to structural stability, pore homogeneity, and wall channeling.

Various in-process synthesis conditions, such as the mass ratio of monomers, polymerization time, concentration of initiator, porogen type and composition, and temperature, affect the molecular arrangement of microglobules and cluster of globules during polymer formation; this confers unique physicochemical characteristics that affect the functions of the polymer at the molecular or nanoscale level.[20–22] The polymerization temperature is critical to the control of the molecular organization of microglobules during synthesis. Hence, it is essential to manipulate the structural and physical characteristics of polymethacrylate monoliths.[14,22] Mihelic *et al.*[23] studied the kinetics of polymerization for methacrylate monolith synthesis and the overall heat of reaction with differential scanning calorimetry. They reported the presence of two heating effects during polymerization: endothermic heat from porogen evaporation and exothermic heat from monomer polymerization with the initiator. However, the endothermic heat of porogen evaporation had minimal effects on the peak temperature of the polymerization process. In addition, it was demonstrated that the thermal polymerization of a monomer–porogen mixture without an initiator can occur but at temperatures above 110 °C.[23] Danquah *et al.*[24] also demonstrated that the mechanism of homogeneous pore formation during polymethacrylate synthesis could be controlled by the minimization of the extent of release of exothermic heat into the polymerization mixture. They accomplished this by expelling the heat of decomposition from the initiator and isothermally pumping free radicals into the monomer mixture for the commencement of monolith synthesis. However, correlations existing between the thermomolecular mechanisms of the synthesis process, and the structural and pore characteristics of the polymer are not well understood. This represents a major research gap. In contrast to the breadth of bioseparation applications of the polymethacrylate monoliths reported, there has been limited work investigating the in-process characteristics, such as the temperature distribution and its impacts on the structural properties of the polymer under various compositional scenarios. In this study, we attempted to develop the theoretical framework essential for understanding the temperature-induced behaviors of the polymerization process and the effects of the in-process synthesis mechanisms on the physicochemical characteristics of the polymer. We formulated an understanding of the polymerization kinetics and evaluated the effects on the rate of polymerization and temperature control. Thermochemical analyses were performed with a real-time technique for the *in situ* parametric characterization of the monolith synthesized by thermal free-radical copolymerization. In addition, a mathematical approach based on reaction kinetics and Avrami's isothermal model was used to establish and monitor the rates of the monomeric reaction after initiation and polymer formation out of the liquid phase.

EXPERIMENTAL

Materials

Glycidyl methacrylate (GMA; molecular weight = 142.15, 97%), ethylene glycol dimethacrylate (EDMA; molecular weight = 198.22, 98%), benzoyl peroxide (BPO; molecular weight = 242.23, 70%), methanol (high performance liquid chromatography grade, molecular weight = 32.04, 99.93%), 1-dodecanol (molecular weight = 186.33, 98%), and cyclohexanol (molecular weight = 100.16, 99%) were purchased from Sigma–Aldrich. Rimless test tubes ($12 \times 15\ cm^2$, Borosil, India) were applied for the *in situ* thermomolecular characterization of monoliths in a water bath (Memmert, Germany). The thermomolecular characterization of the synthesis processes was carried out with a real-time midi logger GL220 thermocouple probe (Graphtec).

Methods

Polymethacrylate Monolith Synthesis. Polymethacrylate resin was produced after the mixture of the monomers (GMA and EDMA), porogens (1-dodecanol and cyclohexanol), and initiator (BPO) for each set of experiments was sonicated for 10 min, sparged with N_2 for 5 min to deoxygenate the mixture and prevent any side reactions that could occur because of the presence of oxygen gas, and held at a constant temperature above the decomposition temperature of the initiator. Thermal free-radical copolymerization was achieved with an isothermal water bath reactor. Because the porogens were mostly nonreactive and were mainly responsible for the solvation of monomers and the medium for pore formation, a fixed ratio (70%:30%) of total porogen to total monomer was maintained throughout the study. Also, the porogenic ratio of cyclohexanol to 1-dodecanol was maintained at 70%:30%. Hence, the polymerization conditions that we changed to represent each set of experiments were the following: temperature, concentration ratio of the functional monomer (GMA) to the crosslinking monomer (EDMA), and concentration of the initiator. The polymerization temperatures investigated for the *in situ* characterization of the synthesis process were 61, 65, 75, and 85 °C at a constant GMA to EDMA ratio of 70%:30% and an initiator concentration of 1% w/v of the total monomer concentration. The ratio of GMA to EDMA

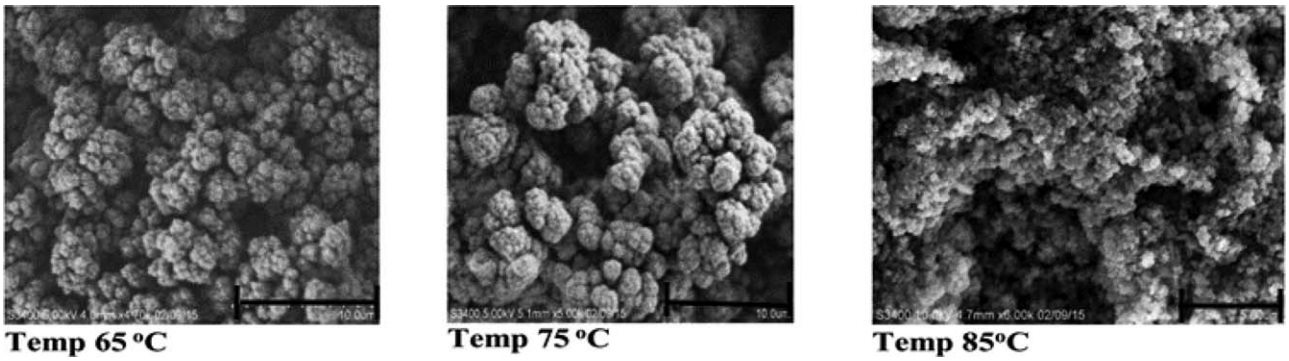

Figure 1. SEM images of polymethacrylate monoliths at magnifications of 4700 × (10 μm), 5000 × (10 μm), and 6000 × (5 μm) at a voltage of approximately 5 kV.

was investigated over the range 30%:70% to 70%:30% at a constant temperature of 85 °C and an initiator concentration of 1% w/v of the total monomer concentration. Variations in the concentration of the initiator from 1 to 3% were also studied at a constant temperature of 85 °C and a GMA to EDMA ratio of 70%:30%.

Temperature Monitoring. Solutions (15 mL) of the previously described mixtures were pipetted into labeled glass test tubes and securely clamped. The clamped test tubes containing the mixtures were then inserted into the water bath while the temperature was monitored in real time with a midi Logger GL220 thermocouple. The monitoring of the results was terminated after the peak temperature was obtained and thermal equilibrium with the water bath was reached. Polymeric monoliths are poor conductors of heat; hence, a continual dip in temperature was observed once the thermal probe continued to be present in the monolith after the thermal equilibrium point.

Scanning Electron Microscopy (SEM) Analysis. With the exception of monoliths used for the *in situ* characterization studies, all other monoliths were washed with methanol in a Soxhlet extractor for a period of about 5 h and air-dried for 7 days for pore characterization. The morphology of the monolithic pores was probed with a variable pressure scanning electron microscope (model S-3400N, Hitachi, Japan). The monoliths were sputter-coated with gold at a sputter current of 20 mA for 30 s to ensure the conduction of signals during probing.

Mathematical Analysis of the Rate of Polymerization. MATLAB and Simulink R 2014b were used to model the polymerization of the monoliths on the basis of a two-phase mechanistic approach deduced from the established Avrami's model for crystallization. The choice of this approach was based on the fact that the formation of bulk monoliths is preceded by nucleation and the reaction of these nuclei with the monomers. The first phase involved the postinitiation monomeric reaction stage to an intermediate liquid polyresin. The second phase involved the transformational processes that led to the formation of a solid polymer from the liquid intermediate phase. Various monomer ratios (1, 1.5, 2, 2.5, and 3) were, therefore, modeled with two different hypothetically selected rate constants of 0.5 and 0.3 s^{-1}.

RESULTS AND DISCUSSION

Effect of the Polymerization Temperature

The lowest polymerization temperature was selected with reference to the decomposition temperature of the initiator (60 °C). As shown in the SEM images in Figure 1, increasing the polymerization temperature resulted in decreases in the pore size [65 °C (4700×, 10 μm), 75 °C (5000×, 10 μm), and 85 °C (6000×, 5 μm)] and increases in the surface area of the adsorbent monolith. In addition, the kinetics of molecular collision increased at elevated temperatures, and this enhanced the energy levels of the reactant species to achieve an activation complex. Under such high-frequency collision conditions, the formation rate of microglobules and their aggregation to globules were hindered by the thermomolecular instability existing in the monomeric phase. The images indicate the decreasing size of the globular assembly with increasing temperature, and this affected the intraglobular and intercluster pore sizes. This observation was in line with previously reported findings.[14,22,25]

An increase in the polymerization temperature led to the rapid decomposition of the initiator into free radicals to form a large number of nuclei per second for a unit volume of the polymerization mixture. From eq. (1), we deduced that an increase in the temperature resulted in an exponential increase in the rate of change of the reaction; this had a direct effect on the amount of free radicals released:

$$\frac{d}{dt} = (1-\xi)^n A \exp\left(-\frac{E_a}{RT_s}\right) \quad (1)$$

where ξ is the extent of the reaction, A is the pre-exponential factor, n is the order of the reaction, E_a is the activation energy, R is the gas constant, and T_s is the polymerization temperature for the synthesis reaction.[23]

Notably, the rate of decomposition of the initiator was directly affected by the polymerization temperature. Because of the rapid increase in the rate of decomposition of the initiator, large amounts of monomers were successively converted in a chain reaction per unit time for every temperature rise. This stepwise conversion and the addition of monomeric units led to the gradual agglomeration and crosslinking of large amounts of nuclei layer by layer until the entire monomeric substrate was converted and polymerized out of the porogenic phase, as illustrated in Figure 2. Also, the rate at which the solid polymer

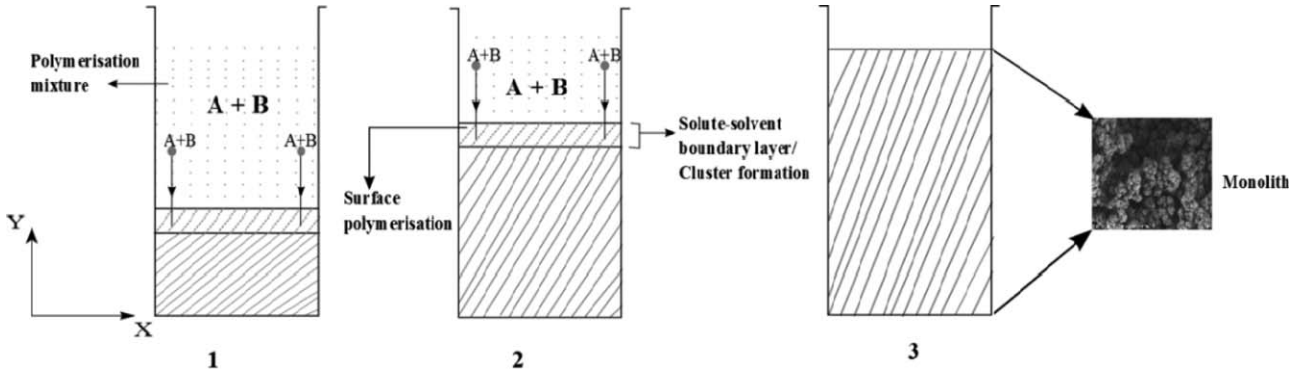

Figure 2. Mechanistic scheme for polymethacrylate monolith formation from the reaction of monomers A and B from the bottom to the top of the mold in a stepwise direction (stages 1–3).

phase crystallized out of the porogenic phase was faster with increasing temperature. This indicated that temperature was a critical parameter affecting the stage-wise molecular mechanisms controlling the overall polymerization process and, thus, the sensible heat transfer into the polymerization mixture, the initiator decomposition rate for the formation of free radicals, the rate of monomeric interactions in the presence of free radicals to form nuclei and microglobules, the aggregation of microglobules to form globules and clusters, and the rate of crystallization of the polymer out of the porogenic phase.

The real-time temperature profiles recorded during polymerization at 61, 65, 75, and 85 °C and presented in Figure 3 showed comparable thermal paths before a polymerization time (t) of 250 s or less. The thermal effects of the process during this period corresponded to sensible heat transfer from the heating medium to the monomeric mixture; this resulted in a warming-up phase until sufficient heat energy was accumulated to commence initiator decomposition into free radicals. The rate of sensible heat dispatch into the monomer medium was a function of the polymerization temperature. The amount of free radicals released after initiator decomposition and, consequently, the rate of formation of nuclei increased per unit time for each increase in the polymerization temperature. High-temperature conditions resulted in fast kinetic interactions between the reacting molecules with a high probability of nuclei formation; this was driven by the availability of free radicals. The amount of heat energy required by the reactant molecules to achieve activation complex was augmented by exotherms released from the initiator decomposition. The release of exotherms resulted in a rapid increase in the polymerization temperature before the process of polymer formation decreased and stabilized. This is shown in Figure 3, which shows the real-time temperature profiles and the corresponding differential profiles. In addition, as the temperature within the mold approached the set polymerization temperature, there was a gradual decline in the rate of change to the value before the peak temperature. The polymerization temperature decreased afterward before it equilibrated at the set-point temperature. A further decline in the polymerization temperature below the set point was observed after polymer formation, and this was attributed to the poor thermal conductivity of the polymer, which obstructed the conductive heat transfer from the heating medium to the thermocouple sensor surface. The respective peak polymerization temperatures (T_ps) recorded were 61.3 °C (for $T_s = 61$ °C), 67.3 °C (for $T_s = 65$ °C), 80.2 °C (for $T_s = 75$ °C), and 96.3 °C (for $T_s = 85$ °C). Set-point temperatures of 61 and 65 °C resulted in small changes in the peak temperature because the amount of exotherms released after initiation was not large enough to cause a significant upsurge in the polymerization temperature. The temperature and overall heat within the monolithic mold during polymerization could be expressed as follows:

$$T_p = T_s + \Delta T \tag{2}$$

$$\Delta H_p = \Delta H_i + \Delta H_{mi} + \Delta H_m \tag{3}$$

where T_s is the set-point temperature, ΔT is the temperature rise at any time after initiator decomposition and the reactions, ΔH_p is the enthalpy change of the polymerization reaction, ΔH_i is the enthalpy change during initiation, ΔH_m is the enthalpy change as the monomers react, and ΔH_{mi} is the enthalpy change as the initiator interacts with the monomers.

Porogens are usually nonreactive during the polymerization process. A previously investigated mixture of porogens (48% cyclohexanol, 12% dodecanal) and monomers (24% GMA, 16% ethylene dimethacrylate) was obtained with a Mettler-Toledo differential scanning calorimeter by Mihelic *et al.*[23] The estimated heat of polymerization, the apparent E_a, and A according to Mihelic *et al.*[23] for the said composition were 190 J/g ± 5%, 1.681 × 10^9 s^{-1}, and 81.5 kJ/mol, respectively. As observed from the aforementioned eqs. (2) and (3), the heat of polymerization was dependent on (1) the set-point temperature, (2) composition of the polymerization mixture, and (3) the thermochemical properties of the monomers because their enthalpies were dependent on their specific heat capacities.

Once the temperature of the reaction mixture reached 60 °C or higher, the initiators underwent complete decomposition to form radicals and released a quantum of energy termed ΔH_i. These radicals reacted sporadically with the subunits of the monomers to form monomer radicals, which also reacted with each other to form smaller chains of polymer units. This led to the formation of monoliths and their associated energies, ΔH_{mi}

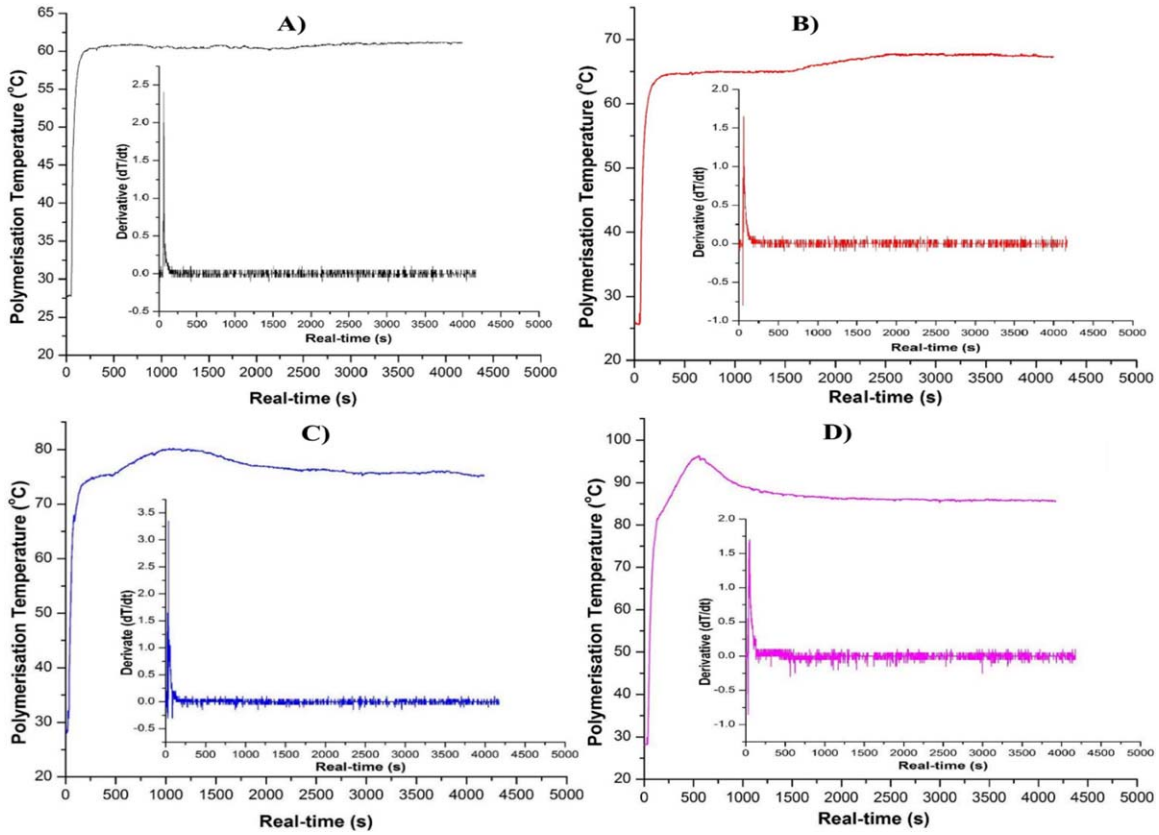

Figure 3. Real-time polymerization temperature profiles for the polymethacrylate monolith synthesis of a volume of 15 mL at different temperatures: (A) 61, (B) 65, (C) 75, and (D) 85 °C. [Color figure can be viewed in the online issue, which is available at wileyonlinelibrary.com.]

and ΔH_m, respectively. Fundamentally, the formation of these monomer radicals and monomer chains through their molecular interactions caused an increase in the energy of the mixture and a temperature rise.

Effect of Monomer Variation

Two types of monomers were used in the synthesis of the polymethacrylate monolith at a constant temperature of 85 °C: EDMA as the crosslinking monomer and GMA as the functional monomer harboring the epoxy moiety. An increase in the concentration of the crosslinking monomer resulted in the formation of a higher number of interconnectivities between the globules and clusters of globules. Nevertheless, excessive ratios of total monomers to total porogen in the nonsolvating mixture could lead to the formation of gel-like monoliths, regardless of the temperature of polymerization and the polymerization time. This is made evident in Figure 4 with 30% total porogen and 70% total monomers synthesized at 85 °C [Figure 4(A)] and 80 °C [Figure 4(B)], respectively.

The type and concentration of the crosslinking monomer defined the network structure of the monolith, affecting physical properties such as the mechanical strength and porosity. High crosslinker concentrations were commensurate with the formation of large surface areas, fewer pores, and a high tensile strength in the polymer. Figure 5 shows the SEM images of the polymethacrylate monoliths synthesized at 40% (6000×, 5 μm), 60% (6000×, 5 μm), and 70% (7000×, 5 μm) EDMA concentrations.

During thermochemical analysis of the polymerization reaction, the ratio of EDMA to GMA was varied from 30 to 70%. The boundary ratios (30–70%) were selected because the polymethacrylate monoliths required reactive epoxy groups in the polymer architecture from the GMA for adsorbent functionalization. Also, very low concentrations of EDMA significantly reduced the mechanical stability of the monolith. From Figure 6, we inferred that an increase in the EDMA/GMA ratio resulted in an increase in the temperature buildup during polymerization.

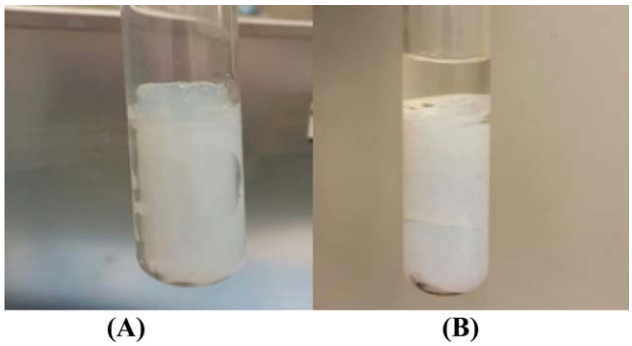

Figure 4. Effects of excess concentrations of the monomers in the porogenic mixture on polymer formation. [Color figure can be viewed in the online issue, which is available at wileyonlinelibrary.com.]

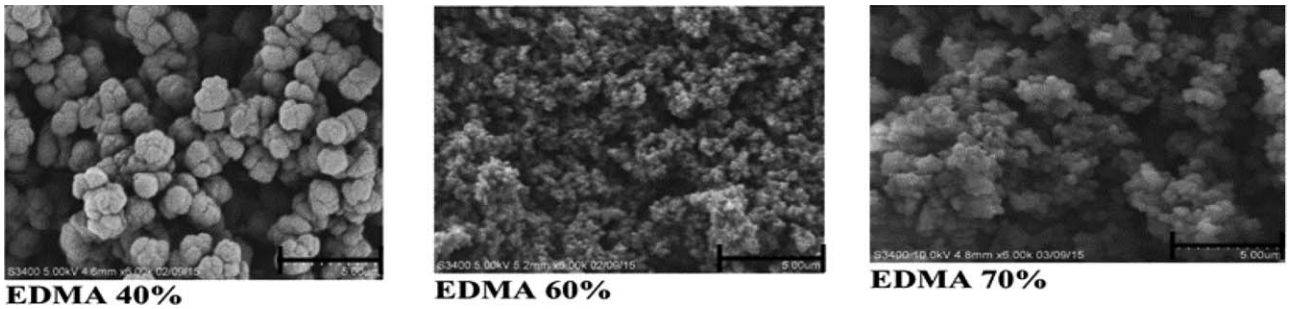

Figure 5. SEM images of polymethacrylate adsorbents synthesized at EDMA concentrations of 40 (5 μm), 60 (5 μm), and 70% (5 μm). SEM analyses were conducted at 5, 5, and 10 kV with magnifications of 4.6 mm at 6000×, 5.2 mm at 6000×, and 4.3 mm at 7000×, respectively.

The peak temperature increased from 96.3 °C at 30% EDMA to 114.3 °C at 70% EDMA. Increasing the EDMA concentration created an additional thermal evolution from the interactions between the generated free radicals and the monomer. In addition to the increased interconnectivities associated with high EDMA concentrations, the increasing peak temperatures further buttressed the point at which elevated EDMA concentrations led to the early formation of nuclei and reductions in the pore size and pore volume.[22] Polymerization systems with various EDMA concentrations generated similar thermal effects, as we observed when the polymerization set-point temperature was increased. However, because the polymerization temperature was kept constant at 85 °C, the thermal paths of the reactions in the sensible heat-transfer region appeared to be similar until the postinitiator decomposition, where the temperature peaked after traversing the polymerization set-point temperature. Under high EDMA conditions, more methylene units were available to react with the free radicals present in the same volume of polymerization mixture. Because of the associated increase in the temperature, which was proportional to the concentration of EDMA, the rate of initiation was also directly affected, and this resulted in late-phase separation.

Effect of the Initiator Concentration

Although it was experimentally determined by Mihelic *et al.*[23] with a differential scanning calorimeter that the synthesis of poly(glycidyl methacrylate-*co*-ethylene glycol dimethacrylate) monoliths can occur at high temperatures greater than 110 °C without an initiator, the latter served as a catalyst to speed up molecular interactions between the monomers, and this enhanced the rate of nucleation. The initiator decomposed at the initiation temperature to form free radicals, which interacted with the monomers to induce nucleation. The free-radical-induced nucleation step required a lower amount of heat to generate significant exotherms after decomposition. The effects of five varied initiator concentrations on the polymerization kinetics and temperature buildup were investigated at a constant EDMA/GMA monomer ratio of 30%:70%, a temperature of 85 °C, and a total porogen concentration of 70% (70% cyclohexanol/30% dodecanal). As shown in Figure 7, the thermal reaction paths before initiation were comparable with an increase in the peak temperature for higher initiator concentrations. The peak temperature increased from 90.7 °C for 1% w/v BPO to 106.3 °C for 3% w/v BPO. In addition, an increase in the initiator concentration resulted in a rapid rate of nuclei formation because more free radicals were released per quantum unit of energy, and this caused the formation of a large number of nuclei in the polymerization mixture. The increase in peak temperatures, together with the rapid polymerization rates, was a result of an increase in the initiator decomposition and produced more radicals, which also reacted with the monomers to produce heat.

The significantly large amount of exotherms released as a result of the increase in the concentration of initiators in the reacting

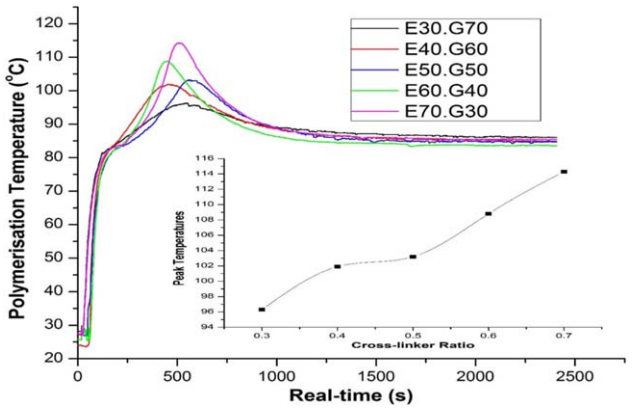

Figure 6. Real-time polymerization temperature profiles for various EDMA/GMA concentration ratios. [Color figure can be viewed in the online issue, which is available at wileyonlinelibrary.com.]

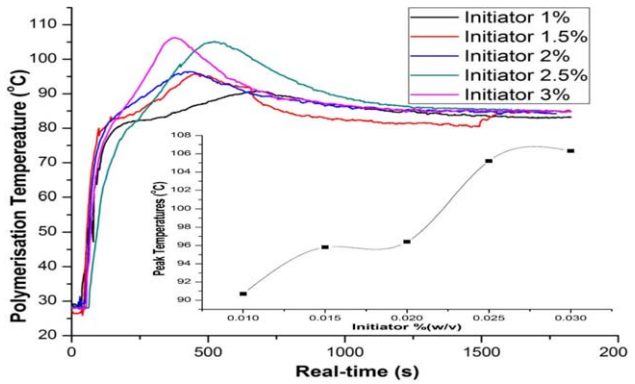

Figure 7. Real-time polymerization temperature profiles for various initiator concentrations. [Color figure can be viewed in the online issue, which is available at wileyonlinelibrary.com.]

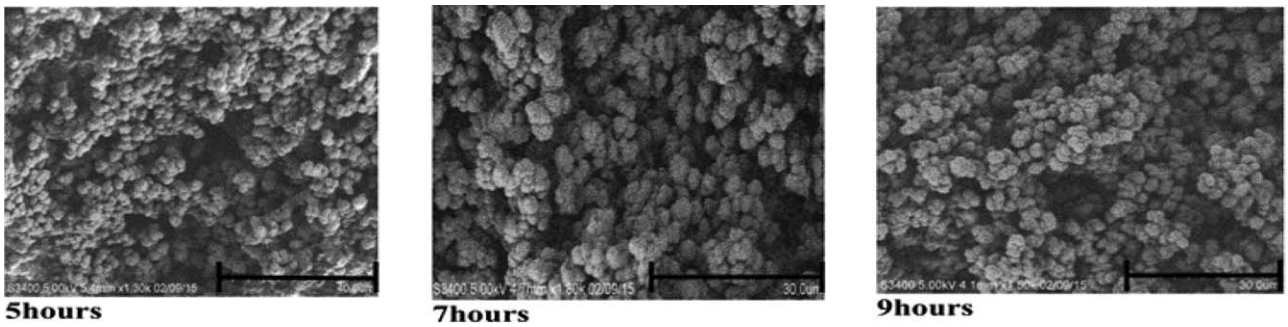

Figure 8. SEM images of polymethacrylate adsorbents synthesized for 5 (40 μm), 7 (30 μm), and 9 h (30 μm). Analyses were performed at resolutions of 5.4 mm at 1300×, 4.2 mm at 1900×, and 4.1 mm at 1500 × at approximately 5 kV.

mixture led to a faster frequency of nucleation formation. This resulted in the formation of more intraglobules and interclusters of globules and smaller pore sizes. Large amounts of initiators also rendered the polymeric monolith highly brittle.

Effect of the Polymerization Time

The polymerization time was another important tool for engineering the structural characteristics of the monolithic adsorbent without changing the synthesis conditions. In this study, different postinitiation polymerization times were investigated for the synthesis of poly(ethylene glycol dimethacrylate-*co*-glycidyl methacrylate). These durations were based on the time during which the polymerization mixture changed from pale white to opaque. We observed that with an increase in the polymerization time from 5 to 9 h, the average pore size decreased from 40 to 30 μm, as shown in Figure 8. The reduction in pore size was due to the continuous conversion of the crosslinker monomers to form more nuclei units, which increased the surface area of the polymer and caused a reduction in the pore size. Internal heat effects within the mold also caused further reductions in the pore size as a result of the low thermal diffusivity of the polymer to the external environment (water bath) after formation. It was previously reported that extending the polymerization time caused decreases in the porosity, height of the monolith, and pore size distribution.[26] We also inferred that the polymerization time coupled with temperature buildup from the bottom of the mold caused a variation in the axial pore size distribution, with smaller pores below the monolith length. Although it was not investigated in this study, we anticipated that there was an optimum time, above which there was no reduction in the pore size of the monolith, and that this optimum time was a function of the concentration of the crosslinker monomer present in the polymerization mixture.

Kinetics of Polymerization

The synthesis of polymethacrylate monoliths by free-radical polymerization is often governed by the reactivity of two monomers (crosslinkers and functional monomers) in a mixture containing an initiator to commence the formation of nuclei after the initiator decomposition temperature is reached. The polymer formation is characterized by two key processes: the chemical reaction between the monomers and the growth of nuclei. Until the sporadic formation of nuclei, no solid phase evolves within the polymerization mixture. The randomized combinations of nuclei to form microglobules and subsequent combinations to form globules and clusters result in the heterogeneous nature of polymethacrylate monoliths and dictate the pore size distribution of the monolith. The degree of randomness can be controlled via the synthesis conditions, such as the temperature and initiator concentration. The nuclei serves as the seed crystal to induce polymer growth. To elucidate the polymer growth process, we applied a crystallization rate model, and the resistance to the formation of the bulk solid polymer phase was factored through the kinetics of the reaction. The two monomers reacted after initiation when subjected to suitable thermochemical conditions. The instantaneous reaction of A and B after initiation resulted in the formation of a viscous liquid intermediary stage containing nuclei subunits; this dictated the propagation of chain molecules in the polymerization process. The extent of the GMA-*co*-EDMA chains influenced the rate of formation of the solid polymer. Figure 9 shows a mechanistic view of the polymer formation process incorporating the reactivity stage and the polymer growth stage. The monomeric reaction stage can be represented by the following chemical reaction:

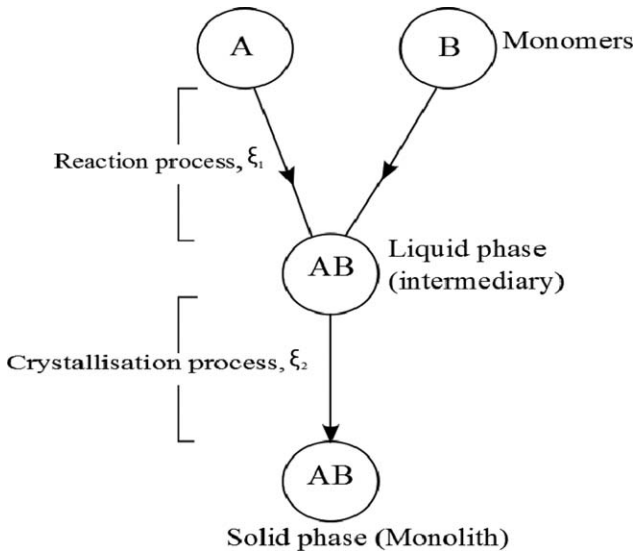

Figure 9. Mechanistic view of polymethacrylate monolith formation showing the monomeric reaction stage and the polymer growth phase. The reaction stage was characterized by ξ_1, and the polymer growth stage was characterized by ξ_2.

$$\underset{(\mathrm{GMA})}{\mathrm{A}} + \underset{(\mathrm{EDMA})}{\mathrm{B}} \xrightarrow{z} \underset{(\mathrm{ploymer})}{\mathrm{AB}} \quad (4)$$

where Z represents the totality of suitable reaction conditions. From eq. (1), Mihelic *et al.*[23] experimentally determined the reaction order for the synthesis of polymethacrylate monoliths as first order. Hence, the reaction rate equation can be written as follows:

$$\frac{d\xi_1}{dt} = k_1(A_0 - \xi_1)(B_0 - \xi_1) \quad (5)$$

where ξ_1 is the extent of formation of the AB_l (intermediary liquid phase), k_1 is the rate constant for the monomeric reaction stage, and A_0 and B_0 are the initial concentrations of the reactants. With the assumption that A_0/B_0 is x and A is the limiting reactant, eq. (5) can be written in terms of the limiting reactant as follows:

$$\frac{d\xi_1}{dt} = k_1(A_0 - \xi_1)(xA_0 - \xi_1) \quad (6)$$

The polymer growth phase occurs gradually in a layer-by-layer format from the bottom of the mold after the formation of the first nuclei to form globules, clusters of globules with pore interconnectivities to yield a single continuous piece. Avrami's isothermal crystallization equation was used to model the polymer growth phase because of its ability to predict the kinetics of polymer formation in a finite volume at isothermal and nonisothermal conditions as follows[27–29]:

$$\frac{d\xi_2}{dt} = k_2 k_2(T) \times f(\xi_2) \quad (7)$$

$$f(\xi_2) = r(1 - \xi_2)[-\ln - \xi_2]^{1-\frac{1}{r}} \quad (8)$$

where ξ_2 is the extent of AB_l liquid transformation into the bulk solid polymer, $k_2(T)$ is the specific rate constant, $f(\xi_2)$ is a function of the extent of the reaction and governs the kinetics of polymer growth, and r is the Avrami's constant, which typically ranges from 1 to 4. A value of $r = 4$ was chosen because the mechanism of polymethacrylate monolith formation is based on the sporadic formation of nuclei. An isothermal model was used because the polymerization temperature rapidly equilibrated to the set-point temperature after initiation. Considering the two stages, monomer reactivity and polymer growth, during the polymerization process, we inferred ξ_1 in the intermediate region was dependent on the rate at which the monomers reacted. Also, ξ_2 was dependent on the amount of AB_s (solid phase monolith) present in the mold.

Various conditions were selected for modeling with MATLAB with different hypothetical conditions on the basis of experimental observations. The ratios of the monomers (A/B) were varied from 1:1 to 3:1 with Avrami's model. Different hypothetical rate constants are also shown in Figure 10 for the two stages leading to the formation of the monoliths.

k_2 represents the rate constant for the polymer growth phase. Theoretically, three scenarios could occur between the monomer reactivity and the polymer growth rates. These scenarios were $k_1 > k_2$, $k_1 = k_2$, and $k_1 < k_2$. Scenario 1 ($k_1 > k_2$) shows the condition where the rate constant of AB_l liquid formation is higher than that of AB_s solid formation. Scenario 2 ($k_1 = k_2$) shows the condition where the rate of AB_l liquid formation is equal to that of AB_s (solid) formation. Scenario 3 ($k_1 < k_2$) shows the condition where the rate of AB_l liquid formation is slower than that of AB_s (solid) formation.

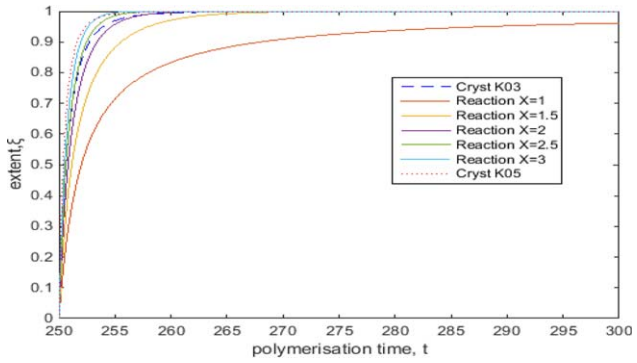

Figure 10. Effects of the polymer growth rate constant and various monomer concentration ratios on the extent of polymerization within the mold. [Color figure can be viewed in the online issue, which is available at wileyonlinelibrary.com.]

In scenario 1, $k_1 > k_2$ was modeled with hypothetical values of 0.5 and 0.3 s^{-1} for k_1 and k_2, respectively, and we observed that the rate at which the monomers reacted to form the intermediary phase was much slower than the rate at which the bulk solid began to form under the same conditions. However, the extent to which the monomers reacted to form the intermediary phase was higher in the early phase of the reaction than that during the formation of the solid phase. Apparently, this section of the Avrami's model was in keeping with the polymerization of the monoliths. Thus, the magnitude of their rate constants at either phase dictated the extent to which the reaction proceeded. The higher the rate constant were for the first stage (the monomeric reaction to form the intermediary AB_l), the higher the amount of AB_l was that could be simultaneously produced for the second stage. According to Avrami's equation [eq. (7)], the formation of the bulk solid phase in the second phase was governed by $f(\xi_2)$; this implied that the rate constants directly affected the ξs.

In scenario 2, where k_1 (0.3 s^{-1}) = k_2 (0.3 s^{-1}), we observed that the rate at which the monomers reacted to form the intermediary phase was faster than that of the formation of the solid phase but with a lower ξ, as was evident in a comparison of the reaction curve at $x = 1$ to that of Avrami's crystallization model ($k = 0.3$). From the analysis, an increase in the ratio of monomers from $x = 1$ to $x = 3$ yielded a corresponding increase in ξ. This was comparable to mixtures with low concentrations of monomers in the porogenic system. The implication was that in the formation of monoliths based on the crystallization model, the rate at which the solid phase forms was mainly temperature dependent because the rate constant was a function of the temperature. In addition, with the same conditions, the transformation rate of the liquid phase into the solid phase to form the bulk polymer was faster. Last, the third scenario, $k_1 < k_2$, was the reverse of the first scenario. Inference from the analysis (graph not shown) indicated that once the rate constant of phase 1 was less than that of phase 2, ξ for phase 1 would be lower than that of the second phase.

CONCLUSIONS

In summary, various conditions for the synthesis of the monoliths were probed to elucidate their *in situ* thermochemical effects during polymerization. Inferences from our parameteric analysis further proved the fact that the key parameter in the control of the pore size and rate of formation hinged on the overall impact of the contribution of the temperature in the polymerization mold. The higher the amount of exotherm released during polymerization was, the smaller the size of the pores was. Online observations from the illustrated data indicated that an increase in the amount of crosslinker (EDMA) from 30 to 70% was correlated with an increase in the polymerization peak temperature from 96.3 to 114.3 °C and a reduction in the pore size, as revealed by the SEM analysis. Similarly, an increase in the concentration of the initiator (BPO) from 1 to 3% w/v resulted in a temperature increase from 90.7 to 106.3 °C. In addition, different set-point temperatures for the water bath resulted in different thermal paths for polymerization mixtures with the same compositions and a corresponding increase in the peak temperatures. Consequently, the overall internal thermal path for the reactive mixture was a function of the amounts of crosslinker and initiator present and the set-point temperature for the water bath.

The moderation of the time as an in-process parameter with constant mixture compositions for the EDMA-*co*-GMA polymeric monoliths also proved to be essential in reducing the pore sizes. An attempt to model the polymerization of the monoliths on the basis of the established Avrami's isothermal model was in keeping with known experimental observations. The rate of monolith formation was observed to intensify with increasing amount of monomers. Essentially, results from the experiment show that the thermochemical processes leading to the formation of the monoliths were very sensitive and could potentially cause variations in the pore size, porosity, rate of formation, and mechanical strength when altered slightly. In addition, the extents of reaction in each phase of the proposed model are directly dependent on their rate constant.

ACKNOWLEDGMENTS

The authors thank the Curtin Sarawak Research Institute for providing financial support for this research through the Curtin Flagship scheme. The authors declare that there is no conflict of interest or anything commercial with respect to this publication.

REFERENCES

1. Svec, F. *J. Sep. Sci.* **2004**, *27*, 747.
2. Wang, H.; Ou, J.; Lin, H.; Liu, Z.; Huang, G.; Dong, J.; Zou, H. *J. Chromatogr. A* **2014**, *1367*, 131.
3. Danquah, M. K.; Forde, G. M. *J. Chem. Technol. Biotechnol.* **2007**, *82*, 752.
4. Nischang, I. *J. Chromatogr. A* **2013**, *1287*, 39.
5. Svec, F. *J. Chromatogr. A* **2012**, *1228*, 250.
6. Podgornik, A.; Yamamoto, S.; Peterka, M.; Krajnc, N. L. *J. Chromatogr. B* **2013**, *927*, 80.
7. Pfaunmiller, E.; Paulemond, M.; Dupper, C.; Hage, D. *Anal. Bioanal. Chem.* **2013**, *405*, 2133.
8. Roberts, M. W.; Ongkudon, C. M.; Forde, G. M.; Danquah, M. K. *J. Sep. Sci.* **2009**, *32*, 2485.
9. Podgornik, A.; Smrekar, V.; Krajnc, P.; Strancar, A. *J. Chromatogr. A* **2013**, *1272*, 50.
10. Ongkudon, C. M.; Danquah, M. K. *J. Chromatogr. B* **2010**, *878*, 2719.
11. Svec, F. *J. Chromatogr. A* **2010**, *1217*, 902.
12. Schlemmer, B.; Bandari, R.; Rosenkranz, L.; Buchmeiser, M. R. *J. Chromatogr. A* **2009**, *1216*, 2664.
13. Vonk, R.; Wouters, S.; Barcaru, A.; Vivó-Truyols, G.; Eeltink, S.; Koning, L.; Schoenmakers, P. *Anal. Bioanal. Chem.* **2015**, *407*, 3817.
14. Szumski, M.; Buszewski, B. *J. Sep. Sci.* **2009**, *32*, 2574.
15. Alves, F.; Scholder, P.; Nischang, I. *ACS Appl. Mater. Interfaces* **2013**, *5*, 2517.
16. Zhang, A.; Ye, F.; Lu, J.; Zhao, S. *Food Chem.* **2013**, *141*, 1854.
17. Aydoğan, C. *J. Chromatogr. A* **2015**, *1392*, 63.
18. Jandera, P.; Staňková, M.; Škeříková, V.; Urban, J. *J. Chromatogr. A* **2013**, *1274*, 97.
19. Yang, R.; Pagaduan, J.; Yu, M.; Woolley, A. *Anal. Bioanal. Chem.* **2015**, *407*, 737.
20. Kim, N.-J.; Kwon, J.-H.; Kim, M. *J. Phys. Chem. C* **2013**, *117*, 15402.
21. Chen, L.; Ou, J.; Liu, Z.; Lin, H.; Wang, H.; Dong, J.; Zou, H. *J. Chromatogr. A* **2015**, *1394*, 103.
22. Danquah, M. K.; Forde, G. M. *Chem. Eng. J.* **2008**, *140*, 593.
23. Mihelic, I.; Krajnc, M.; Koloini, T.; Podgornik, A. *Ind. Eng. Chem. Res.* **2001**, *40*, 3495.
24. Danquah, M. K.; Ho, J.; Forde, G. M. *J. Appl. Polym. Sci.* **2008**, *109*, 2426.
25. Svec, F.; Fréchet, J. M. *J. Macromolecules* **1995**, *28*, 7580.
26. Svec, F.; Fréchet, J. M. *J. Chem. Mater.* **1995**, *7*, 707.
27. Piorkowska, E.; Galeski, A. *Physics* **2003**, *42*, 773.
28. Avrami, M. *J. Chem. Phys.* **1941**, *9*, 177.
29. Foreman, J.; Blaine, R. *Annu. Tech. Conf.* **1995**, *2*, 2409.